Mesenchymal stem cells and neural crest stem cells from adult bone marrow: characterization of their surprising similarities and differences

Wislet-Gendebien, Sabine ; Laudet, Emerence ; Neirinckx, Virginie ; Alix, Philippe ; Leprince, Pierre ; Glejzer, Aneta ; Poulet, Christophe ; Hennuy, Benoit ; Sommer, Lukas ; Shakhova, Olga ; Rogister, Bernard

Abstract: The generation of neuronal cells from stem cells obtained from adult bone marrow is of significant clinical interest in order to design new cell therapy protocols for several neurological disorders. The recent identification in adult bone marrow of stem cells derived from the neural crest stem cells (NCSC) might explain the neuronal phenotypic plasticity shown by bone marrow cells. However, little information is available about the nature of these cells compared to mesenchymal stem cells (MSC), including their similarities and differences. In this paper, using transcriptomic as well as proteomic technologies, we compared NCSC to MSC and stromal nestin-positive cells, all of them isolated from adult bone marrow. We demonstrated that the nestin-positive cell population, which was the first to be described as able to differentiate into functional neurons, was a mixed population of NCSC and MSC. More interestingly, we demonstrated that MSC shared with NCSC the same ability to truly differentiate into Tuj1-positive cells when co-cultivated with paraformaldehyde-fixed cerebellar granule neurons. Altogether, those results suggest that both NCSC and MSC can be considered as important tools for cellular therapies in order to replace neurons in various neurological diseases.

DOI: https://doi.org/10.1007/s00018-012-0937-1

Mesenchymal stem cells and neural crest stem cells from adult bone marrow: characterization of their surprising similarities and differences.

Sabine Wislet-Gendebien[1*], Emerence Laudet[1*], Virginie Neirinckx[1], Philippe Alix[1], Pierre Leprince[1], Aneta Glejzer[1], Christophe Poulet[2], Benoit Hennuy[6], Lukas Sommer[3], Olga Shakova[3], Bernard Rogister[1,4,5] .

[1] University of Liege, GIGA Neurosciences, CHU B36, 1 Avenue de L'hôpital, 4000 Liège, Belgium
[2] University of Liege, GIGA Research, CHU B34, 1 Avenue de L'hôpital, 4000 Liège, Belgium
[3] Institute of Anatomy, University of Zurich, CH-8057 Zurich, Switzerland.
[4] University of Liège, GIGA Development, Stem Cells and Regenerative Medicine
[5]Department of Neurology, CHU Liège, Belgium
[6]University of Liege, GIGA Genomics Plateform, CHU B34, 1 Avenue de L'hôpital, 4000 Liège, Belgium

* Those two authors equally contributed to this work

Corresponding Author:

Sabine Wislet-Gendebien
s.wislet@ulg.ac.be
Phone: +32-4-3665956
Fax: +32-4-3665912

Running title:

Characterization of neural crest and mesenchymal stem cells from adult bone marrow

Author contribution:

SWG : conception – design – collection of data – data analysis – manuscript writing
EL : collection of data – data analysis – final approval of manuscript
PA : collection of data
VN : collection of data
AG : collection of data
CP : collection of data – data analysis – manuscript writing
BH : collection of data – data analysis
OS : Provision of study material
LS : Provision of study material - final approval of manuscript
PL: design- collection of data – data analysis – final approval of manuscript
BR : Conception – design – Financial support – data analysis - final approval of manuscript

Key words

Neural crest stem cells; mesenchymal stem cells; adult bone marrow; cell fate; microarray

ABSTRACT

The generation of neuronal cells from stem cells obtained from adult bone marrow is of significant clinical interest in order to design new cell therapy protocols for several neurological disorders. The recent identification in adult bone marrow of stem cells derived from the neural crest (NCSC) might explain the neuronal phenotypic plasticity shown by bone marrow cells. However, little information is available about the nature of these cells compared to mesenchymal stem cells (MSC), their similarities and differences. In this paper, using transcriptomic as well as proteomic technologies, we compared NCSC to MSC and stromal nestin-positive cells, all of them isolated from adult bone marrow. We demonstrated that the nestin-positive cell population, which was the first to be described as able to differentiate into functional neurons, was a mixed population of NCSC and MSC. More interestingly, we demonstrated that MSC shared with NCSC the same ability to truly differentiate into Tuj1-positive cells when co-cultivated with paraformaldehyde-fixed cerebellar granule neurons. Altogether, those results suggest that both NCSC and MSC can be considered as important tools for cellular therapies in order to replace neurons in various neurological diseases.

INTRODUCTION

Symptoms in human neurological disorders such as Parkinson's disease, Huntington's disease, amyotrophic lateral sclerosis (ALS), Alzheimer's disease, multiple sclerosis (MS), stroke, and spinal cord injury are a consequence of a loss of neurons and glial cells in the brain or spinal cord. Cell replacement strategies should provide a basis for the development of new highly efficient symptomatic therapies for a broad spectrum of human neurological diseases. However, the paucity of suitable cell types for cell replacement therapy in patients suffering from neurological disorders has hampered the development of this promising therapeutic approach [1]. The recent finding that adult bone marrow contains neural crest-derived cells rebooted the cellular therapy challenges as those cells can be easily isolated and can give rise to different type of mature neural cells. However, several points still need to be clarified before using those cells in such a cellular therapy protocols. In particular, one may ask whether the neuronal phenotypic plasticity of the bone marrow cells is an exclusive property of these neural crest-derived cells.

In early vertebrate development, the neural crest is specified in the embryonic ectoderm at the boundary of the neural plate and the ectoderm. Once specified, the neural crest cells (NCC) undergo a process of epithelial-to-mesenchymal transition (EMT) that will confer them the ability to migrate. The EMT involves different molecular and cellular machineries and implies deep changes in cell morphology and in the type of cell surface adhesion and recognition molecules. After completing EMT, the NCC delaminate from the epithelial neural folds/neural tube and start migrating along characteristic pathways to differentiate into a wide variety of derivatives [2].

In 2000, Jiang et al. developed a two-component genetic system based on Cre/lox recombination to label indelibly the entire mouse neural crest population at the time of its

formation, and to detect its progeny at any time thereafter [3]. In such a model, the fate of NCC was mapped *in vivo* by mating *ROSA26* Cre reporter (*R26R*) mice, expressing β-galactosidase upon Cre-mediated recombination, with mice expressing Cre recombinase under the control of the *Wnt1* promoter. Using this transgenic model, Sieber-Blum and Grim demonstrated the presence of pluripotent neural crest-derived cells in adult hair follicles [4], Wong et al. identified NCC in mouse adult skin [5] and Nagoshi et al. isolated NCC from adult bone marrow [6]. Another mouse expressing the Cre recombinase under the control of the P0 promoter is also used in the same approach to map the NCC and, in the bone marrow, both Cre expressing mice have allowed to tag the same neural crest-derived cells [7-9].

In this paper, using the *Wnt1-Cre/R26R* double transgenic mice model, as previously described, we confirmed the presence of neural crest-derived cells in adult bone marrow. As only little information could be found on neural crest-derived cells from adult bone marrow, we decided to further characterize those cells by comparing them to the nestin-positive cell population initially described as a neurogenic population. Indeed, we demonstrated several years ago that only nestin-positive cells isolated from adult bone marrow could differentiate into functional neurons [10, 11]. Working with cell clones, we performed a direct comparison of neural crest stem cells (NCSC) and mesenchymal stem cells (MSC), both isolated from adult bone marrow. Altogether, this study highlighted the fact that bone marrow nestin-positive population was a mixed population, mainly composed of NCSC, but containing also few MSC. More surprisingly, we demonstrated that MSC were able to truly differentiate (without fusion process) into neural cells when placed in appropriate culture conditions.

MATERIAL AND METHODS

Animal care.

Wnt1-Cre/R26R-LACZ double transgenic mice were used to confirm the presence of neural crest cells in adult bone marrow and to discriminate NCSC clones from MSC clones. Transgenic green fluorescent protein (GFP) C57BL/6J mice as well as wild type C57BL/6J mice (The Jackson Laboratory, Bar Harbor, Maine, http://www.jax.org) were used to produce cerebellar granule neurons (CGNs). Adult (8–15-weeks-old) rats (The Jackson Laboratory, Bar Harbor, Maine, http://www.jax.org) were used to compare nestin-positive and nestin-negative cell populations. Rodents were bred at the University of Liège Central Animal facility and euthanized in accordance with the rules set by the local animal ethics committee as well as the Swiss Academy of Medical Sciences.

Bone marrow stromal cell (BMSC) culture. Adult (8–15-weeks-old) rat bone marrow was obtained from femoral and tibial bones by aspiration and was resuspended into 5 ml of Dulbecco's modified Eagle's medium (DMEM; Invitrogen, Merelbeke, Belgium, http://www.invitrogen.com). Between 100 and 200 x 10^6 marrow cells were plated on 175-cm^2 tissue culture flasks in DMEM added with 10% (v/v) fetal bovine serum (FBS; Invitrogen). After 24 hours, the non-adherent cells were removed. Bone marrow cells from adult (8–15-week-old) mice were obtained from femoral and tibial bones by aspiration and were resuspended in 5 ml of MesenCult Medium (StemCells Technologies, Grenoble, France, http://www.stemcell.com). After 24 hours, non-adherent cells were removed. When the BMSCs became confluent, they were resuspended using 0.05% trypsin-ethylenediaminetetraacetic acid (EDTA) (Invitrogen) and then sub-cultured (750,000 cells / 5 ml).

Preparation and culture of Mouse cerebellar granule neurons. Mouse cerebellar granule neurons (CGNs) were prepared from 3-days-old GFP or wild type C57BL/6J mice (The

Jackson Laboratory, Bar Harbor, ME, USA, http://www.jax.org), [11]. Green mice express green fluorescent protein (GFP) under control of the β-actin promoter [11]. Wild-type CGNs were only used with NCSC clones as those clones would express LacZ, which was used to discriminate both cell types. Briefly, cerebella were removed and freed of meninges. They were then minced into small fragments and incubated at 37°C for 25 minutes in 0.25% trypsin and 0.01% DNAse (w/v, in a cation-free solution). Fragments were then washed with minimum essential medium (MEM; Invitrogen) supplemented with glucose (final concentration 6 g l^{-1}), 5 µg ml^{-1} insulin (Sigma-Aldrich, St. Louis, MO, USA, http://www.sigmaaldrich.com;), 1 mM sodium pyruvate (Invitrogen) and 10% horse serum (Invitrogen). The potassium concentration was increased to 25 mM, while the sodium concentration was decreased in an equimolar amount (MEM-25HS). The dissociation was achieved mechanically by up-and-down aspirations in a 5-ml plastic pipette. The resulting cell suspension was then filtered on a 15-µm nylon sieve. Cells were then counted and diluted to a final concentration of $2.5x10^6$ cells ml^{-1}. The cell suspension was finally plated on a substrate previously coated with 0.1 mg ml^{-1} polyornithine. The cells were cultured for 24 hours before any other experimental procedure was performed.

Clonal selection. Passage 5 BMSC (from *Wnt1-Cre/R26R*-LACZ double transgenic mice) have been seeded in a 96 wells plate at a dilution of 0.7 cell / well, in MesenCult Medium (Stem Cells Technologies) When cells reached confluence, they were dissociated with 0,05% trypsin-EDTA and sub-cultured at 150,000 cells ml^{-1}.

Immunocytofluorescence. Briefly, cell cultures were fixed with 4% paraformaldehyde (PFA) for 10 minutes at room temperature, then blocked with 10% normal donkey serum (NDS) and/or 3% bovine serum albumin (BSA) for 45 minutes. Anti-Sox10 (1:200; Affinity Bioreagents, CO, USA, www.antibodydirectory.com), anti-nestin (1:300; Novus Biologicals, Littleton, CO, USA www.novusbio.com/), anti-GFAP (1:1000; DakoCytomation, Glostrup,

Denmark, http://www.dako.com), anti-Tuj1 (1:1000; Covance, Princeton, NJ, USA http://www.covance.com), anti-SMA (1:400; Sigma-Aldrich), anti-MAP2ab (1:1000; Sigma-Aldrich), anti-TRP2 (1:400; Abcam, Cambrige, UK, http://www.abcam.com/), and anti-$p75^{NTR}$ (1:100; Millipore, Billerica, MA, USA, http://www.millipore.com/) were used for 2 hours at room temperature or over-night at 4°C. After four washes, FITC- or rhodamine-conjugated secondary antibodies (1:500; Jackson Immunoresearch Laboratories) were incubated for 1 hour at room temperature and finally, cell cultures were counterstained with Vectashield HardSet Mounting Medium with DAPI (Vector Laboratories, Burlingame, http://www.vectorlabs.com). Preparations were observed using an Olympus laser scanning confocal microscope (Olympus, Tokyo, http://www.olympus-global.com). The fraction of positive cells was determined by counting ten non-overlapping microscopic fields for each coverslip (with a minimum of three coverslips per experiment) in at least three separate experiments (n represented the number of experiments).

Other Stainings. X-gal staining was performed on 2% PFA-fixed cells. Cells or bone sections were incubated for 2 hours in PBS supplemented with 20 mM Tris (pH 7.4), 2 mM $MgCl_2$, 0.02% NP-40, 0.01% Na-deoxycholate, 5 mM $K_3Fe(CN)_6$ (Sigma-Aldrich), 5 mM $K_4Fe(CN)_6$ (Sigma-Aldrich), and 1mg ml^{-1} 1-Methyl-3-indolyl-β-D-galactopyranoside (Sigma–Aldrich) in dimethylsulfoxide (DMSO). The reaction was stopped by phosphate-buffered saline (PBS) washes.

Functional characterization. Several protocols have been used to analyze the differentiating abilities of bone marrow neural crest cells into smooth muscle cells, adipocytes, osteocytes, chondrocytes and melanocytes. Smooth muscle differentiation: Cells were incubated in DMEM/F12 supplemented with B27 (Invitrogen), Chick Embryo Extract 5% and 1 nM transforming growth factor β (TGF-β; PeproTech, London, United Kingdom, http://www.peprotech.com). Adipogenic differentiation: differentiation was induced by

treatment with DMEM containing 0,5 mM 1-methyl-3-isobutylxanthine (Sigma-Aldrich), 1 µM dexamethasone (Sigma-Aldrich), 0.01 mg ml^{-1} bovine insulin, 0.2 mM indomethacin (Sigma-Aldrich). Cells were placed in the above adipocyte induction medium for 21 days. The differentiation was evaluated by accumulation of lipid vacuoles and staining with Oil Red O (Sigma-Aldrich) following fixation with 4% PFA. Melanocyte formation was obtained after 10 days in MEM containing 10% FBS, 50 ng ml^{-1} murine stem cell factor (mSCF; PeproTech) and 100 nM endothelin-3 (Sigma-Aldrich). Cells were fixed with 4% PFA and stained with an anti-TRP2 antibody. For osteogenic induction, cells were cultivated in StemXVivo Osteogenic media (R&D Sytems, Minneapolis, MN, USA, http://www.rndsystems.com). Osteogenic differentiation was measured using p-nitrophenyl phosphate, a substrate for alkaline phosphatase (Sigma-Aldrich). Level of alkaline phosphatase activity was detected by development of soluble yellow reaction product that may be read at 405 nm using a Thermo Labsystems Multiskan Ascent 354 (Lab Recyclers, Gaithersburg, MD, USA, http://www.labrecyclers.com). Chondrocyte formation was obtained after 1 month in DMEM containing 0.1 µM dexamethasone (Sigma-Aldrich), 1 mM sodium pyruvate (Invitrogen), 50 µg ml^{-1} ascorbic-2-phosphate acid (Sigma-Aldrich), 6.25 µg ml^{-1} transferin (Sigma-Aldrich), 6.25 µg ml^{-1} bovine insulin, 6.25 µg ml^{-1} selenic acid (Sigma-Aldrich), 5.35 µg ml^{-1} linoleic acid (Sigma-Aldrich), 1.25 mg ml^{-1} BSA and 10 ng ml^{-1} TGF-β3 (PeproTech). Pellets were fixed with 4% PFA, paraffin-embedded, cut as 5 µm sections and stained with toluidine blue. In each case, medium was refreshed every 3 – 4 days.

Neural differentiation ability. Several protocols have been used to differentiate MSC and NCSC into GFAP- or Tuj1-positive cells: 1) *Serum-containing medium:* Neural differentiation has been monitored by cells in DMEM/F-12 supplemented with 10% FBS (Invitrogen) for 10 days. 2) *Neurotrophin-containing medium*: Neural differentiation was

observed after culture of cells in DMEM/F12 supplemented with B27 (Invitrogen), 1% FBS, 50 ng ml^{-1} brain-derived neurotrophic factor (BDNF; PeproTech), 50 ng ml^{-1} nerve growth factor (NGF; PeproTech) and 10 ng ml^{-1} neurotrophin-3 (NT-3; PeproTech) for 2 weeks. 3) *Co-culture with mouse cerebellar granule neurons*: 12500 NCSC or MSC were co-cultivated with CGNs (prepared as previously described), for 5 days in serum-free CGN culture medium.

Signaling pathway inhibition. For neural differentiation inhibition, two clones were separately co-cultivated with CGNs for 5 days, in presence of 1 μM PD98059 (Sigma-Aldrich) and 1 μM SB431542 (Sigma-Aldrich) inhibitors dissolved in DMSO. Inhibitors were placed at day 0 of co-culture and medium supplemented with inhibitors was replaced after 3 days. Each inhibitor effect was compared to DMSO control conditions. Culture coverslips were processed to immunocytofluorescence and preparations were observed using an Olympus laser scanning confocal microscope (Olympus, Tokyo, Japan, http://www.olympus-global.com). The fraction of positive cells was determined by counting ten non-overlapping microscopic fields for each coverslip (with a minimum of three coverslips per experiment) in at least three separate experiments (n represented the number of experiments).

RNA extraction, RT-PCR analyses. Total RNA was prepared using the RNeasy total RNA purification kit (Qiagen, Valencia, CA, http://www.qiagen.com). cDNA synthesis was carried out using Moloney-murine leukemia virus (MMLV) Reverse transcriptase (Promega) and random hexamer primers (Promega), following the manufacturer's instructions. PCR procedures and primers have been described in Glejzer et al., [9].

Microarray analysis. The RNA quality was assessed by the Experion automated electrophoresis system using the RNA StdSens Analysis Kit (Bio-Rad, Nazareth, Belgium http://www.Bio-Rad.com). Four micrograms of total RNA were labeled using the GeneChip

Expression 3'-Amplification One-Cycle Target Labeling Kit (Affymetrix, Santa Clara, CA, USA, http://www.affymetrix.com) following the manufacturer's protocol. The cRNA was hybridized to GeneChip Mouse Genome 430 2.0 (Affymetrix) according to the manufacturer's protocol. Briefly, double-stranded cDNA was synthesized from 4 µg of total RNA primed with a poly-(dT)-T7 oligonucleotide. The cDNA was used in an *in vitro* transcription reaction in the presence of T7 RNA polymerase and biotin-labeled modified nucleotides for 16 h at 37°C. Biotinylated cRNA was purified and then fragmented (35–200 nucleotides) together with hybridization controls and hybridized to the microarrays for 16 h at 45°C. Using Fluidics Station (Affymetrix), the hybridized biotin-labeled cRNA was revealed by successive reactions with streptavidin R-phycoerythrin conjugate, biotinylated anti-streptavidin antibody, and streptavidin R-phycoerythrin conjugate. The arrays were finally scanned with an Affymetrix/Hewlett-Packard GeneChip Scanner 3000 7G. The data were generated with the PLIER algorithm included in Affymetrix GeneChip Command Console Software (AGCC) and Expression Console. The probe sets have been filtered on signal log ratio (greater than 0.6 for upregulated and less than –0.6 for downregulated transcripts) and on *P* value associated with the change status (<0.001 for up-regulated probe sets, >0.999 for down-regulated probe sets). To determine which pathways were significantly regulated, lists of expressed genes were uploaded in Ingenuity Pathway Analysis software (IPA 6.0; Ingenuity Systems; http://www.ingenuity.com). Microarray results from NCSC and MSC clones are accessible on GEO datasets / NCBI (GSE30419; http://www.ncbi.nlm.nih.gov/gds).

Dendrogramme was generated in an unsupervised analysis comparing expression array data of NCSC clones, MSC clones, with several expression array data available from the Gene Expression Omnibus database (Edgar et al., 2002; GEO) http://www.ncbi.nlm.nih.gov/geo/. All samples from GEO datasets have been processed on Affymetrix Mouse Genome Expression Set 430 GeneChips. Normalization and data filtering were performed using BRB-

ArrayTools software version 3.8.1 developed by Dr. Richard Simons and the BRB-ArrayTools Development Team, http://linus.nci.nih.gov./BRB-ArrayTools.html. We used the GCRMA algorithm as normalization step. Quartiles of each expression arrays were compared in a boxplot view. Medians, first and third quartiles were similar in each case (data not shown). This similarity allowed the comparison of the 118 arrays under the same analysis process. Background noise has been removed with the "Log Intensity variation" function of "BRB-ArrayTools" at a p-value > 0.05. The package "pvclust" (Ryota Suzuki & Shimodaira., 2009) from R-cran (Team, R.D.C., R: A Language and Environment for Statistical Computing; 2009) was used on the remaining filtered genes to build and test the architecture of each cluster of samples. "pvclust" is used for assessing the uncertainty in hierarchical cluster analysis. For each cluster in hierarchical clustering, p-values are calculated via multiscale bootstrap resampling. This indicates how strong the cluster is supported by data. "pvclust" provides two types of p-values: AU (Approximately Unbiased) p-value in red and BP (Bootstrap Probability) value in green. AU p-value, which is computed by multiscale bootstrap resampling, is a better approximation to unbiased p-value than BP value computed by normal bootstrap resampling. We choose the most commonly used "Euclidean distance" as dissimilarity metric and three different methods of linkage (single, complete, average) to obtain dendrogram structures. The relevance of dendrograms architecture was then tested by data permutations. We set the multiscale boostrap resampling argument of "pvclust" at 1000 permutations of genes to test those dendrograms. Only the "average linkage" method showed the best stable structure (figure 4).

2D-DIGE analyses and Mass spectrometry 2D-DIGE proteomic analysis has been performed on proteins from rat MSC. Proteins were extracted in a lysis buffer containing 7 M urea (GE Healthcare, Chalfont St. Giles, United Kingdom, http://www.gehealthcare.com), 2 M thio-urea (GE Healthcare), 30 mM Tris (pH 8.5) (GE Healthcare) and 2% ASB14 (Sigma-

Aldrich). The supernatant containing the extracted proteins was precipitated (2-D Clean-Up Kit, GE Healthcare) and amounts of resolubilized proteins were determined using RC-DC Protein Assay (Bio-Rad). Each 25 µg of sample protein was labeled with 200 pmol CyDye (GE Healthcare), either Cy3 or Cy5, and left for 30 min in the dark. The labeling reaction was stopped by adding 10 mM lysine for 10 minutes at 4°C. An internal standard was prepared by mixing equal quantities of all the experimental samples and was labeled with Cy2. Then all the samples within the experiment were mixed in pairs together with 25 µg of the labeled internal standard and were separated by isoelectric focusing using pH 3-11 (24 cm) IPG strips in an Ettan IPGphor focusing system (GE Healthcare) in the first dimension. The following electrophoresis steps were successively applied: 8 hours of rehydration, 1 hour at 500 V, 1 hour to 1000 V (gradient), 3 hours to 8000 V (gradient) and 8 hours 45 min at 8000 V (step-and-hold). Before initiating the second dimension step, proteins in IPG strips were reduced for 15 min in an equilibration buffer (50 mM Tris-HCl (pH 8.8), 6 M urea, 30 % glycerol, 2 % SDS) containing 1% DTT and then they were alkylated in the same equilibration buffer containing 5% iodoacetamide. IPG strips were placed on top of classical 12,5 % SDS-PAGE gels and the electrophoretic migration was completed in an Ettan Dalt apparatus (GE Healthcare) at 2.5 W/gel for 30 minutes, and then 25 W for 4 hours. After scanning the gels in a Typhoon 9400 Laser Scanner (GE Healthcare) at three different wavelengths corresponding to the different CyDyes, 2-D gel analysis software (DeCyder version 6.5, GE Healthcare) was used for spot detection, gel matching and spot quantification relative to the corresponding spot in the internal standard. Protein spots that showed a significant variation in their abundance of at least 2 fold (Student T-test, $p<0.05$) were selected for further BVA analysis (Biological Variation Analysis) and then they were automatically picked from the gels with the Ettan Spot Picker (GE Healthcare) and subjected to automatic tryptic digestion (PROTEINEER dp automated digester, Bruker Daltonics, Bremen, Germany,

http://www.bdal.com). Gel pieces were washed three times in 50 mM NH_4HCO_3 followed by 50% (ACN ??) ACN/50 mM NH_4HCO_3. Two other washes were carried out with 100% ACN to dehydrate the gels. In-gel digestion was performed with freshly activated trypsin (Roche, Basel, Switzerland, http://www.roche.com) at a concentration of 10 ng l^{-1} in 50 mM NH_4HCO_3/5% ACN. After rehydration of the gel pieces at 8°C for 60 minutes, tryptic digestion was carried out at 30°C for 4 hours. The resulting digested peptides were extracted with 1% trifluoroacetic acid (TFA) for 30 minutes at 20°C with occasional shaking. A volume of 3 ml of protein digests was adsorbed for 3 minutes on Prespotted AnchorChip plates with α-Cyano-4-hydroxycinnamic acid (CHCA) as a matrix, using the PROTEINEER dp automat. Then the spots were briefly desalted with 10 mM dihydrogenoammonium phosphate in 0.1% TFA. MS fingerprints of the samples were acquired using the Ultraflex II MALDI-TOF-TOF mass spectrometer (Bruker Daltonics) in the mass range: 700-3500 Da. The (PMF?) (PMFs) were searched against the NCBI database. The variable and fixed modifications were methionine oxidation and cysteine carbamylation, respectively, with a maximum number of missed cleavages of 1. Mass precision tolerance error was set to 100 ppm. Peaks with the highest intensities, obtained in TOF/MS mode, were next analyzed by LIFT MS/MS. Proteins were identified with the Biotools 3.0 software (Bruker Daltonics) using the Mascot search engine (Matrix Science, Boston, MA, USA, www.matrixscience.com).

Electrophysiological Recordings. All NCSC clones or MSC clones were pooled into NCSC or MSC mixed populations, keeping the same ratio of each clone. Mixed populations were than co-cultivated for 5 to 22 days with CGNs, as previously described. During recordings, cover slip was continuously perfused with artificial cerebrospinal fluid (ACSF ; 137 mM NaCl, 5.4 mM KCl, 2 mM CaCl2, 22.2 mM D-glucose and HEPES; pH 7.4) at room temperature. ACSF and drug applications were performed using gravity and a BPS-8 valve control system (ALA scientific, Westbury, NY, www.alascience.com/). 1 µM tetrodotoxin

(TTX ; Tocris Biosciences, Ellisville, MO, http://www.tocris.com) and 20 mM tetraethylammonium (TEA ; Sigma-Aldrich) were added to the ACSF to respectively block Na^+ or K^+ current. Neurons from clones were discriminated using an Axiovert microscope (Zeiss, Oberkochen, Germany, http://www.zeiss.de/). Pipettes were pulled on a P-87 micropipette puller (Sutter Instruments, Novato, CA, Canada, www.sutter.com) using borosilicate glass capillary tubing (2.0 mm OD. 1.16 mm ID; Hilgenberg, Malsfeld, Germany, http://www.hilgenberg-gmbh.com). The resistance of the electrodes was 5-8 MΩ when filled with the intracellular solution: 130 mM KCl, 2 mM $CaCl_2$, 2 mM HEPES, 2.5 mM ATP-Mg, 2.5 mM ATP-Na_2, 10 mM EGTA and 11.1 mM D-Glucose ; pH 7.4. Non-fluorescent neurons (from clones, as CGN were originated from GFP-mice) were sealed at a gigaohm and placed in whole-cell configuration. Membrane potentials and currents were recorded using an EPC9 amplifier (HEKA, Lambrecht/Pfalz, Germany, www.heka.com/) connected to Patchmaster software (HEKA). Liquid junction potentials were corrected. Only recordings in which the series resistance was lower than 30 MΩ and remained stable (variations ≤ 20%) were used. No compensation of the series resistance was performed.

Statistical Analysis. Data were analyzed statistically using Statistica 9 program (StatSoft, Inc., Tulsa, OK, USA, www.statsoft.com). Data are reported as mean ± standard deviation, with the number of experiments (n) between parentheses. Level of statistical significance was set at $p < 0.05$.

RESULTS

1. Transcriptomic comparison of rat nestin-negative versus nestin-positive bone marrow stromal cells. We previously demonstrated that adult rat nestin-positive bone marrow stromal cells isolated from adult bone marrow were able to differentiate into excitable neurons, when co-cultured with mouse cerebellar granule neurons [11]. The proportion of nestin positive-cells in culture was quite low at passage 0, but would increase with reduced cell confluence [12] and higher passage numbers [10], until reaching a plateau (75% nestin-positive cells) at passage 7. As it was not clear if nestin-positive and nestin-negative cells were different cell populations or the same cells at different maturation stages, we decided to further characterize those two types of cells. We compared passage 4 BMSC as nestin-negative cell population and passage 15 BMSC as nestin-positive cell population, both cell types being cultivated for 48 hours in serum-free medium before analyses, as previously described [10]. Microarray analyses revealed that nestin-negative and nestin-positive BMSC expressed around 20000 genes with 379 genes that were significantly different (supplementary data Table S1). Using Ingenuity Pathway Software (IPA 6.0), we classified all expressed genes according to their relevance to cell fate specificity. A total of five categories of genes have been described (stem cell, neural, mesenchymal, hematopoietic and endothelial genes). As we can observe on Figure 1.A and Figure S1 (supplementary data), when compared to nestin-negative cells, nestin-positive cells over-express genes that characterize stem cell and neural cell states and decrease their level of expression of genes involved in mesenchymal, hematopoietic or endothelial cell fate. Likewise, we compared genes involved in signaling pathways mainly expressed by nestin-positive cells compared to nestin-negative cells. Again, using Ingenuity Pathway Software, we classified all expressed genes in 8 families of signaling pathway genes: Wnt/Fzd, Notch/Delta, Insulin, NF-κB, MapK, PI3K, Jak/Stat and TGFbeta. As observed on Figure 1.B and S2 (supplementary

data), the three most regulated gene families were Notch/Delta, Insulin and NF-κB. Although those results were interesting, it was not possible to rigorously answer with the question if nestin-positive and nestin-negative BMSC were different cell populations or cells with different maturation stages. We consequently decided to have a closer look at the two cell populations on a proteomic level.

2. Proteomic comparison of rat nestin-negative (P4) versus nestin-positive (P15) bone marrow stromal cells. Proteomic analyses using the 2D-DIGE technology revealed 131 spots with different abundance (minimum 2 fold-change, Figure 1.C), and identified (by mass spectrometry) 71 proteins that were significantly over-expressed in nestin-positive compared to nestin-negative MSC. As observed on Table 1 (Supplementary data), more than 35% of those proteins are implicated in cell cycle regulation (DARS, ANXA5, ATIC, CALD1, DPYSL2, FTL, HSP90AB1, NEDD4, P4HA1, PDIA6, POLA1, RSP6KA1, SH3GL1, TPM3, VAMP1, CAPNS1, MSN, PAK2, TXNL1, PDIA3 and PRDX3). Although those results would suggest that nestin-positive cells had a more proliferative phenotype and thus were at a more immature stage than nestin-negative cells, it was still not possible to answer the question of different cell populations or different maturation stages. One of the main reasons for this was probably the fact that the data contained a lot of falsely unregulated genes or proteins due to the heterogenous cell populations as nestin-positive cell population (high passages) would still contain 25% of nestin-negative cells and *vice versa*. We consequently decided to use a different approach to answer that question.

3. Confirmation of the presence of neural crest-derived stem cells in mouse adult bone marrow. As several results pointed out that nestin-positive BMSC and NCSC shared common characteristics (i.e. SOX10, ErbB3 and $p75^{NTR}$ over-expression), we formulated the

hypothesis that nestin-positive cells as observed in our cultures could actually be neural crest derived cells. With a paradigm similar to the one used by Nagoshi et al., who recently demonstrated the presence of NCSC in adult bone marrow [6], we verified our hypothesis using a double transgenic model (*Wnt1-Cre/R26R* mice) to track NCSC. Bone marrow stromal cells (BMSC) were first extracted from *Wnt1-Cre/R26R*-LacZ adult mice and cultured in MesenCult® medium. Interestingly, in those culture conditions, the proportion of LacZ expressing cells increased from 5.42% ± 1.68% of cells at passage 2 (P2) to 41.55% ± 16.26% of cells at passage 6 (P6), similarly to what was observed with adult rats and adult mice nestin-positive BMSC (p=0.002, n=3, repeated measure ANOVA followed by Tukey-Kramer's post hoc test; Fig. 2A-C). In order to be able to rigorously compare NCSC with MSC, both isolated from adult bone marrow, we decided to generate clonal cultures using β-galactosidase expression as a reporter gene to discriminate NCSC clones from MSC clones.

4. Clonal analyses of NCSC versus MSC from adult bone marrow. Single cells, from passage 5 BMSC, were placed in a 96-wells plate in MesenCult medium. In those conditions, 1.2% of cells were able to proliferate. Five NCSC clones (β-galactosidase-positive cells) and six MSC clones (β-galactosidase-negative cells) have been maintained in long-term culture (more than 25 passages), showing their stable self-renewal ability. However, all characterization described thereafter have been performed within the first 10 passages after clonal selection. We first characterized those clones for their expression of the classical neural crest markers Sox10, $p75^{NTR}$ and nestin. All NCSC clones were 100% positive for Sox10, $p75^{NTR}$ and Nestin (Fig. 2 D-F). On the other hand, MSC clones were Sox10-negative, 20,2% ± 10,8% of cells (in each clone) were nestin-positive and were weakly positive for $p75^{NTR}$ (Fig. 2H-J). As we rigorously followed the growth of our clones, we were sure that each clone was derived from a single cell, thus heterogenous nestin expression by MSC clones was

probably due to a variable sensitivity to inductive or repressive factors. Indeed, the level of nestin-positive cells increased to around 90% when those cells were placed in serum-free condition (Fig. 2K) similar to what we initially described with high passage non-clonal adult rat and mice BMSC [10]. This sensibility to serum for nestin expression is also a difference between NCSC and MSC as there was no effect on NCSC clones placed in serum-free medium (Fig.2G). Those results and the increase of LacZ expression in high passage numbers BMSC cultures strongly suggested that nestin-positive MSC populations, initially described in 2003 [10], were thus a mixed population of NCSC and MSC, with a majority of NCSC at higher passages. Moreover, those results have been confirmed on general population of BMSC culture isolated from Wnt1-Cre/R26R- LacZ mice, showing that nestin-positive cells were mainly composed of β -galactosidase positive cells, but also containing few β -galactosidase negative cells (data not shown).

5. Multipotency of NCSC compared to MSC. We then analyzed NCSC and MSC clones abilities to differentiate into mesenchymal cells. NCSC clones were able to differentiate into chondrocytes (Fig. 3.B) and melanocytes (Fig. 3.D) but not into adipocytes (Fig. 3.A), smooth muscle cells (Fig. 3.C) or osteocytes (Fig. 3.I), while MSC were able to differentiate into adipocytes (Fig. 3.E), osteocytes (Fig. 3.I), chondrocytes (Fig. 3.F) and smooth muscle cells (Fig. 3.G). The fact that we could not differentiate NCSC clones into adipocytes and smooth muscles was quite surprising as we previously demonstrated that NCSC were also able to differentiate into adipocytes and smooth muscle cells when cultivated in presence of Wnt1 and BMP2 [9], two factors described for maintenance and proliferation of NCSC. Consequently, NCSC clones were pre-treated with Wnt1 and BMP2 for one week before inducing their differentiation [13]. Interestingly, those clones became then able to differentiate into adipocytes (Fig. 3.J), however, we were still unable to differentiate them

into smooth muscles (data not shown). We then analyzed the neural differentiation abilities of NCSC clones compared to MSC clones. We first placed those cells in serum-containing medium (Fig. 3.K-P) for spontaneous differentiation, then in neurotrophin-containing medium for specific differentiation (Fig. 3.Q-T). In those conditions, only NCSC clones were able to differentiate into Tuj1-positive cells. However, both types of clones were able to differentiate into GFAP-positive cells, although this phenomenon was more frequently observed in NCSC clones. As we previously demonstrated that BMSC were able to differentiate into functional neurons when co-cultivated with cerebellar granule neurons (CGNs) [11], we analyzed the abilities of NCSC and MSC clones to differentiate into Tuj1-positive cells using a co-culture protocol. In those conditions, NCSC (Fig.4.A) and MSC (Fig.4.B) were able to differentiate into Tuj1-positive cells after 5 days. At this stage of the study, two hypotheses could explain the absence of neuronal differentiation of MSC in absence of co-culture: 1) several studies have demonstrated that BMSC were able to fuse with neurons to adopt their characteristics [14]. 2) It is possible that neurotrophins or serum were not sufficient factors to orient MSC toward a neuronal fate, and that other factors expressed by CGNs would be necessary. To test the first hypothesis, we cultivated NCSC or MSC clones on PFA-fixed CGNs, in the presence of CGNs conditioned medium, as previously described [11]. Surprisingly, under those conditions, we observed Tuj1-positive cells derived from NCSC as well as MSC clones, suggesting that some MSC were also able to truly differentiate into neural cells (Fig. 4.C-D). To rule out the possible extinction of GFP in PFA-fixed CGN, we placed them for 5 days in conditioned medium in absence of clones, and thus confirmed their stable GFP level (data not shown). We consequently concluded that MSC were not sensitive to neurotrophin stimulation, which could be partially explained by their low amount of $p75^{NTR}$ expression. Finally, to complete the characterization of neuronal differentiation, we performed electrophysiological recordings on NCSC and MSC clones. Using fluorescent microscopy,

we selected cells that exhibited a neuron-like shape (rounded cell body with extended processes), and were clearly GFP negative (see Methods). Whole-cell patch-clamp recordings were obtained from 49 MSC and 43 NCSC that had been co-cultured with CGNs for 5–20 days. No significant differences were observed in term of resting membrane potentials over the time or between cell types : MSC V_{rest} -35 ± 4 mV and NCSC V_{rest} -37 ± 5 mV. Applying hyperpolarizing and depolarizing voltage steps to voltage-clamped cells, from a holding potential of –50mV, assessed the presence of voltage-gated channels. Throughout the culture period, 100% of MSC and NCSC showed outward currents that were blocked by tetraethylammonium (TEA, 20mM), indicating the presence of voltage-gated potassium channels (data not shown). However, 2% of MSC and no NCSC showed tetrodotoxin-sensitive (TTX, 1 μM), fast inward currents, indicating the presence of voltage gated sodium channels (Fig.4.E). Consistent with the occurrence of voltage-gated sodium and potassium currents, injection of positive current pulses in current-clamp mode elicited action potentials in 2% of MSC cells (Fig.4.E) whereas no action potentials could be observed in NCSC. Finally, the expression of neuron-specific cytoskeletal proteins MAP2ab, which was absent after 5 days, was observed after 12 days of co-culture in both MSC and NCSC clones (Fig.4.F).

6. Transcriptomic comparison of NCSC versus MSC clones. To finalize the characterization of NCSC and MSC clones, we performed microarray analyses on those two sets of clones. In this case around 20000 genes were expressed by NCSC and MSC clones with 3169 genes that were significantly up or down-regulated between the two sets of clones (Supplementary data, Table S2). We classified those genes into cell fate gene families (Fig. 5.C). As expected, NCSC clones would mainly over-express neural genes and down-express mesenchymal and endothelial genes (Supplementary data, Fig. S3). We confirmed the

differential expression of several genes between both types of clonal populations by semi-quantitative RT-PCR. NCSC as well as MSC clones were negative for oct4, nanog, rex1, pax3, pax6, sox1, msl1, twist1 and **w**nt1 (data not shown), but, positive for Notch1, nestin, hes1, sox2, CXCR4, $p75^{NTR}$, sox10, id2, snail1, ngn1, and foxd3 (Fig. 5.B). All expressed genes seemed to be over-expressed in NCSC, except snail1 and CXCR4 which were down-regulated. We also compared our microarray results with microarrays data obtained in other studies with different types of cells including cranial NCSC (isolated from embryos), embryonic fibroblasts, MAPC, ES-derived neurons, etc. and built a dendrogramme reflecting the closeness of origin of the different cell types (Fig. 5.A). As a result, MSC clones were still regarded as the closest cell type to the NCSC clones, followed by neural crest cells isolated from head and neck region of embryos and neurons obtained from ES cells. On the other hand, developing heart cells as well as adipose cells shared lesser similarities with NCSC as well as with MSC clones.

Finally, looking at signaling pathways (Fig. 6.A ; supplementary data Fig. S4), genes families that were the most regulated in NCSC clones compared to MSC clones were the TGFβ and MAPK gene families. To test if these two pathways were implicated in neural differentiation of NCSC clones, we co-cultivated those clones with CGNs, in the presence of MAP/ERK inhibitor (PD98059) or TGFβ inhibitor (SB431542). In those conditions, we observed a significant decrease of the number of Tuj1-positive cells treated with the MAP/ERK inhibitor as only 3,7 % ± 1,3 % Tuj1-positive cells were found (Fig. 6.B-E), instead of 10,6 % ± 1,9 % Tuj1-positive cells (control condition). No significant difference was observed after treatment with TGF-β inhibitor as 11,1 % ± 3,5 % Tuj1-positive cells were found. Those results suggest that the MAP/ERK pathway could be one of the main signaling pathways directing NCSC toward a neuronal fate.

DISCUSSION

Several studies have already reported the presence of NCSC in adult bone marrow [6, 8, 9]. Those cells could be good candidates for use in cellular therapy approaches to improve symptoms in various neurological disorders, as they are able to differentiate into neural cells and are found in an easy-access location, allowing autologous graft procedures. However, really few information is known about their characteristics, especially in comparison with MSC. In this study, we first analyzed the nestin-positive cell population isolated from adult rat bone marrow. Indeed, we initially described this population as the neurogenic population of adult bone marrow since only those cells were able to differentiate into functional neurons [11]. However, given that our nestin-positive cell population was not pure (75% of BMSC were nestin-positive in the best conditions), it was difficult to identify specific markers for this population regarding the nestin-negative cells. This was also emphasized by the fact that in a transcriptomic approach, we found that only 379 genes on a total of 20000 were up- or down-regulated between the two populations.

Then, we formulated the hypothesis that this nestin-positive population could actually be constitued by neural crest derived cells. However, this hypothesis was incorrect as clonal analyses revealed that nestin-positive cell population isolated from adult bone marrow was a mixed population of NCSC and MSC. Noteworthy, the regulation of nestin expression was different between MSC and NCSC as serum was able to repress this expression only in MSC, while no serum effect was observed on NCSC. A similar phenomenon has already been described for glial precursor cells in which serum (through TGFβ factors) inhibited nestin expression [15]. Moreover, we previously demonstrated that thrombin was able to up-regulate nestin expression by radial glial cells, but decreased the nestin expression in MSC cell population from bone marrow, indicating that the regulation of nestin expression could be finely modulated in various conditions and/or cell types [12].

Analyzing the mesenchymal differentiation abilities between those two cell types, it appeared that NCSC were able to differentiate into chondrocytes and melanocytes, while MSC were able to differentiate into adipocytes, chondrocytes, and smooth muscles. However, when pre-treated with Wnt1 and BMP2 factors, NCSC acquired the ability to differentiate into adipocytes. Those results were consistent with a recent study realized by John et al., in which Sox10-positive neural-crest derived progenitors were found to be unable to differentiate into adipocytes [16]. Indeed John and collaborators showed that TGFβ1 induced a switch in neural to mesenchymal potential in NCSC. Similarly, several studies have demonstrated that three main classes of signals: Wnts, BMP2/BMP4 and TGFβ1,2,3, directly influence the production of particular neural crest cell fates [17]. Remarkably, we failed to differentiate NCSC into smooth muscle cells. A couple of previous studies demonstrated that NCSC isolated from adult bone marrow could give rise to smooth muscle cells [6-8]. Both studies used Wnt1-Cre/EGFP transgenic mice and cell sorting to isolate NCSC from adult bone marrow based on their EGFP expression. EGFP-positive population was then placed in unspecific conditions (10% serum containing medium) and smooth muscle differentiation was evaluated after few days. In both case, only few SMA-positive cells were observed showing a restrictive capacity of differentiation into smooth muscle. Moreover, none of those studies confirmed the EGFP-expression of SMA-positive cells, which could not rule out a small contamination of NCSC population by MSC. Moreover, a recent study demonstrated that Foxd3 expression by NCSC maintain neural potential and repress mesenchymal fate [22]. RT-PCR analyses confirmed a strong level of expression of Foxd3 gene in NCSC clones compared to MSC clones (Fig. 5), which could also partially explained the absence of smooth muscle differentiation.

Looking at the neural differentiation abilities of NCSC and MSC clones, we observed that NCSC were able to differentiate into GFAP- and Tuj1-positive cells in serum-containing

medium or in neurotrophins-containing medium, as well as in co-culture conditions with CGNs. However, MSC were able to differentiate into GFAP- or Tuj1-positive cells only in the co-culture condition. It is interesting to mention that NGF, BDNF and NT3 receptors are the tyrosine kinase receptors: TrkA, TrkB and TrkC, but also the low affinity nerve growth factor receptor $p75^{NTR}$. Microarray results revealed no expression of Trk receptors by MSC and a low expression level of $p75^{NTR}$, which could explain the absence of effect of neurotrophins on MSC. Those receptors were expressed in NCSC and the signaling pathway that is recruited by these receptors in NCSC could be the MAPK pathway as we demonstrated the genes belonging to this signaling pathway were the most up-regulated in NCSC clones and its inhibition decreased significantly their neuronal differentiation.

As mentioned above, the only way to differentiate MSC into neural cells was the co-culture protocol. To rule out the possibility of cell fusion events, we co-cultivated NCSC as well as MSC on PFA-fixed CGNs, in the presence of medium conditioned by these CGNs. Under those conditions, both cell types were able to differentiate into GFAP- or Tuj1-positive cells, suggesting that both cell types were truly able to differentiate into neural cells. More surprisingly, only MSC were able to fire action potentials in co-culture conditions, even if both cell populations showed some maturation signs, as they would express MAP2ab after 12 days of co-culture. In correlation with the weak number of MAP2ab-positive cells (less than 1%), we observed only a low level of action potentials, suggesting that some factors were missing to complete the full differentiation of MSC or NCSC.. .

On the other hand, MSC were found to be able to differentiate into neuronal cells in the presence of CGNs, suggesting that CGNs expressed factors that are mandatory to direct MSC toward a neuronal fate. Moreover, at least one of those factors is linked to the CGN, membrane as conditioned medium alone was not able to induce their neuronal differentiation. A recent publication revealed that Wnt1 factor induces Tlx3 expression, which was correlated

with neuronal differentiation ability of MSC [19]. Wnt1 is a developmentally important gene involved in intercellular signaling that is expressed by CGNs in newborn mice [20]. Recent publications showed that Frizzled receptors FZD2, 3 and 4 were able to bind Wnt1 [21]. Our microarray results indicate that MSC expressed FZD1, 2, 5, 7 and 8, but not FZD3 and 4 receptors. However, Wnt1 factor seemed to be necessary (but not sufficient) to induce neuronal differentiation of MSC, as Wnt1 treated cells did not spontaneously differentiate into neuronal cells when placed in DEM/F12 medium (data not shown).

In conclusion, this study demonstrated that the putative bone marrow-derived nestin-positive population, which was able to differentiate into functional neurons, was a mixed population, mainly composed of NCSC, but also containing few MSC. More surprisingly, we demonstrated that *bona fide* MSC were able to truly differentiate (without fusion process) into neural cells when placed in appropriate culture conditions that could depend on Wnt signaling pathway activation. However, an interesting question, that remains pending, is the phenotype of the two types of neurons obtained from MSC and NCSC, especially regarding their abilities to synthesize neurotransmitters since this constitutes an essential characteristic in a perspective of cellular therapy for various neurological diseases.

ACKNOWLEDGMENT

This work was supported by a grant from the Fonds National de la Recherche Scientifique (FNRS) of Belgium, by a grant of the Action de Recherche Concertée de la Communauté Française de Belgique, by the Belgian League against Multiple Sclerosis associated with the Leon Fredericq Foundation, and by the Swiss National Science Foundation. PL is a senior research associate of the FNRS. AG is a Marie Curie Host Fellow for Early Stage Research Training, EURON 020589 within the 6th FP of the EU, Marie Curie Actions - Human Resources and Mobility. Normalisation and data filtering were performed using BRB-ArrayTools software version 3.8.1 developed by Dr. Richard Simons and BRB-ArrayTools Development Team http://linus.nci.nih.gov./BRB-ArrayTools.html. Patricia Ernst and Alice Marquet also provided technical assistance to this study. Finally, we would like to thanks Professor Vincent Seutin who gave us the opportunity to use his electrophysiological platform.

REFERENCES

1. Kim SU, de Vellis J. Stem cell-based cell therapy in neurological diseases: a review. J Neurosci Res. 2009;87:2183-2200.
2. Kalcheim C, Burstyn-Cohen T. Early stages of neural crest ontogeny: formation and regulation of cell delamination. Int J Dev Biol. 2005;49:105-116.
3. Jiang X, Rowitch DH, Soriano P, et al. Fate of the mammalian cardiac neural crest. Development. 2000;127:1607-1616.
4. Sieber-Blum M, Grim M, Hu YF, et al. Pluripotent neural crest stem cells in the adult hair follicle. Dev Dyn. 2004;231:258-269.
5. Wong CE, Paratore C, Dours-Zimmermann MT, et al. Neural crest-derived cells with stem cell features can be traced back to multiple lineages in the adult skin. J Cell Biol. 2006;175:1005-1015.
6. Nagoshi N, Shibata S, Kubota Y, et al. Ontogeny and multipotency of neural crest-derived stem cells in mouse bone marrow, dorsal root ganglia, and whisker pad. Cell Stem Cell. 2008;2:392-403.
7. Fujiwara K, Mochida S, Matsui A, et al. Fulminant hepatitis and late onset hepatic failure in Japan. Hepatol Res. 2008;38:646-657.
8. Morikawa S, Mabuchi Y, Niibe K, et al. Development of mesenchymal stem cells partially originate from the neural crest. Biochem Biophys Res Commun. 2009;379:1114-1119.
9. Glejzer A, Laudet E, Leprince P, et al. Wnt1 and BMP2: two factors recruiting multipotent neural crest progenitors isolated from adult bone marrow. Cell Mol Life Sci. 2011;68:2101-2114.
10. Wislet-Gendebien S, Leprince P, Moonen G, et al. Regulation of neural markers nestin and GFAP expression by cultivated bone marrow stromal cells. J Cell Sci. 2003;116:3295-3302.
11. Wislet-Gendebien S, Hans G, Leprince P, et al. Plasticity of cultured mesenchymal stem cells: switch from nestin-positive to excitable neuron-like phenotype. Stem Cells. 2005;23:392-402.
12. Wautier F, Wislet-Gendebien S, Chanas G, et al. Regulation of nestin expression by thrombin and cell density in cultures of bone mesenchymal stem cells and radial glial cells. BMC Neurosci. 2007;8:104.
13. Kleber M, Lee HY, Wurdak H, et al. Neural crest stem cell maintenance by combinatorial Wnt and BMP signaling. J Cell Biol. 2005;169:309-320.
14. Alvarez-Dolado M, Pardal R, Garcia-Verdugo JM, et al. Fusion of bone-marrow-derived cells with Purkinje neurons, cardiomyocytes and hepatocytes. Nature. 2003;425:968-973.
15. Sakai Y, Rawson C, Lindburg K, et al. Serum and transforming growth factor beta regulate glial fibrillary acidic protein in serum-free-derived mouse embryo cells. Proc Natl Acad Sci U S A. 1990;87:8378-8382.
16. John N, Cinelli P, Wegner M, et al. Transforming growth factor beta-mediated Sox10 suppression controls mesenchymal progenitor generation in neural crest stem cells. Stem Cells. 2011;29:689-699.
17. Dorsky RI, Moon RT, Raible DW. Environmental signals and cell fate specification in premigratory neural crest. Bioessays. 2000;22:708-716.

18. **Cragnolini AB, Huang Y, Gokina P, et al. Nerve growth factor attenuates proliferation of astrocytes via the p75 neurotrophin receptor. Glia. 2009;57:1386-1392.**
19. **Kondo T, Matsuoka AJ, Shimomura A, et al. Wnt signaling promotes neuronal differentiation from mesenchymal stem cells through activation of Tlx3. Stem Cells. 2011;29:836-846.**
20. **Fu Y, Tvrdik P, Makki N, et al. Precerebellar Cell Groups in the Hindbrain of the Mouse Defined by Retrograde Tracing and Correlated with Cumulative Wnt1-Cre Genetic Labeling. Cerebellum. 2011.**
21. **Williams JM, Oh SH, Jorgensen M, et al. The role of the Wnt family of secreted proteins in rat oval "stem" cell-based liver regeneration: Wnt1 drives differentiation. Am J Pathol. 2010;176:2732-2742.**
22. **Mundell NA and Labosky PA. Neural crest stem cell multipotency requires Foxd3 to maintain neural potential and repress mesenchymal fates. Development. 2011; 138:641-652**

FIGURES

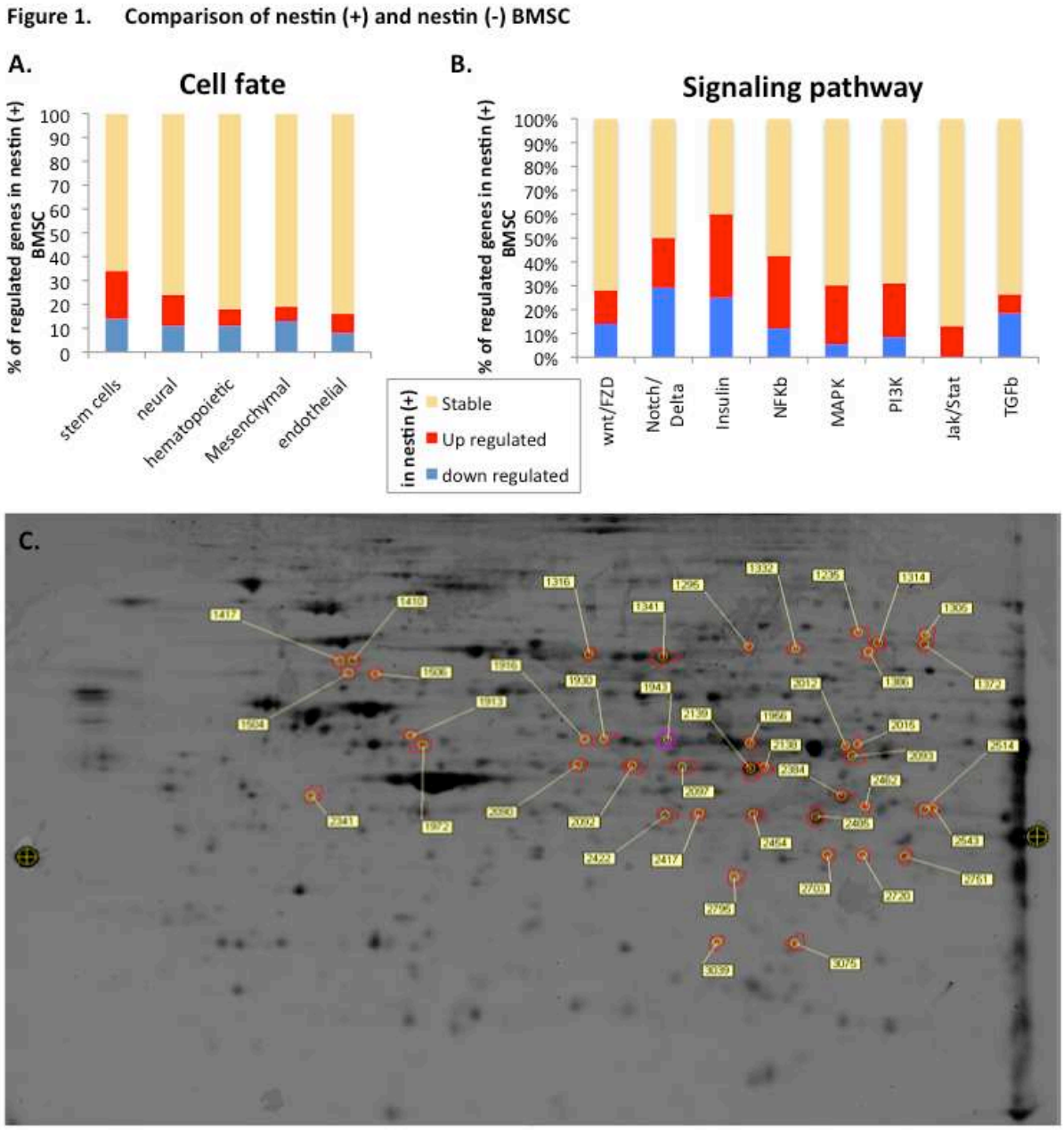

Figure 1. Transcriptomic and proteomic comparison of nestin-positive and nestin-negative MSC isolated from rat adult bone marrow. A. Cell fate. In this figures, we reported all genes that were expressed by nestin-positive or nestin-negative MSC, and involved in cell fate decision. We classified those genes in 5 families: Stem cell, neural, hematopoietic, mesenchymal and endothelial fate. Those results suggested that nestin-

positive MSC population contained a higher percentage of stem cells or cells that would adopt a neural fate. **B. Cell Signaling Pathway.** In this part, we reported all genes that were expressed by nestin-positive or nestin-negative MSC, and involved in cell signaling. We classified those genes in 8 families: WNT/FZD, NOTCH/DELTA, INSULIN, NFkB, MAPK, PI3K, JAK/STAT and TGFbeta. Looking at those results, it appeared that Insulin signaling pathway was the most regulated family of genes, however, MAPK had the highest number of over-expressed genes, suggesting that Insulin and MAPK pathways would be the most activated pathways in nestin-positive MSC. Genes that were equally expressed by both cell types are in yellow, over-expressed genes in red and down-expressed genes in blue. **C. Proteomic comparison**. A representative two dimensional gel electrophoresis protein separation used for determining differentially expressed proteins in nestin-positive and nestin-negative MSC. Contoured spots correspond to proteins of interest that were picked for mass spectrometry identification.

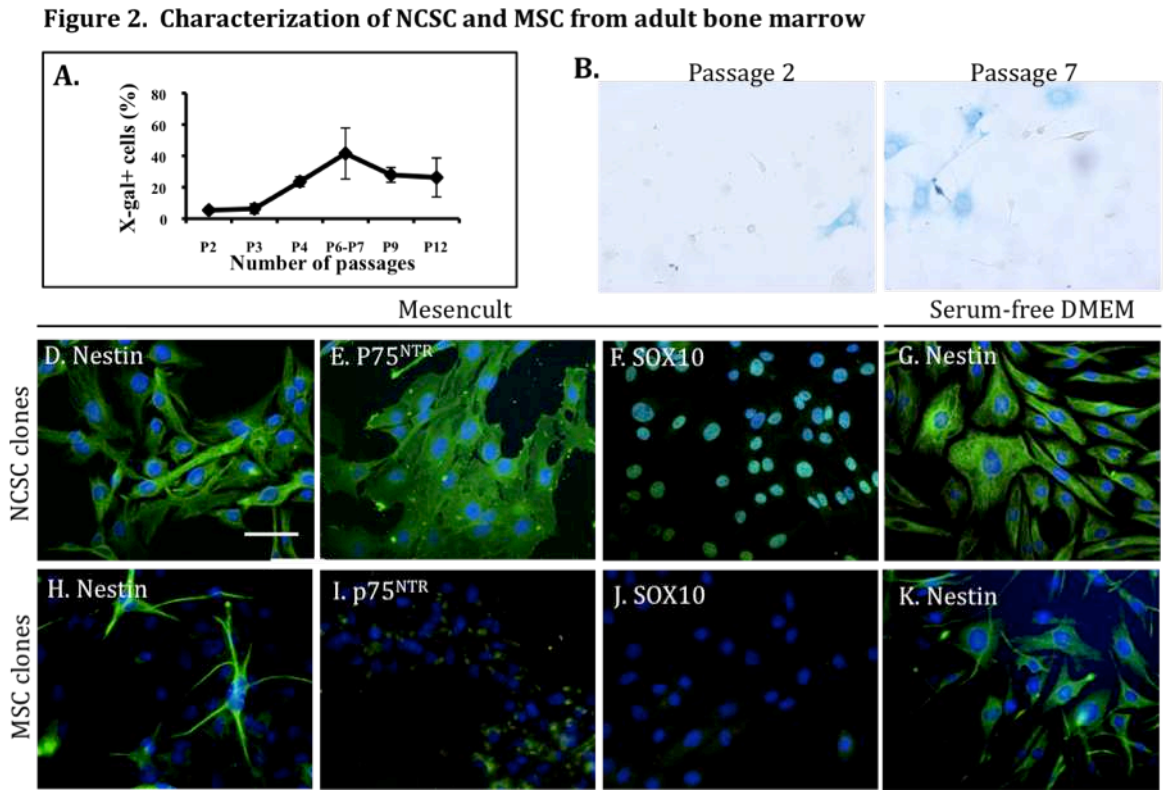

FIGURE 2. Characterization of neural crest cells from mouse adult bone marrow. Adult bone marrow contains NCSC. NCSC were identified within adult BMSC extracted from Wnt1-Cre/R26R mouse femoral bones. **A.** As number of passages (P) increases, a greater proportion of NCC expressing β-galactosidase was observed to reach a maximum at P6–P7 (n = 3, $p < 0.005$, repeated measures ANOVA followed by Tukey-Kramer's post hoc test). **B.** NCSC were identified in P2 and P7 BMSC by X-gal staining. Scale bar = 50µm. **(D-V)** BMSC have been seeded in clonal density (0,7 cell / well in 96 well plates), in Mesencult Medium. In those culture conditions, 1,2 % of cells proliferated as clonal culture. We analysed 5 NCSC clones (identified by the expression of beta-galactosidase) and 6 MSC clones. All NCSC clones were nestin-positive (Green, **D**), p75NTR-positive (green, **E**) and Sox10-positive (green, **F**). 20,2% ± 10,8% of MSC (from each clone) were nestin-positive (green, **H**) and some MSC were weakly positive for $p75^{NTR}$ (green, **I**) and all MSC were negative for Sox10 (**J**). Interestingly, nestin expression was induced in MSC when cells were

cultivated in serum-free medium (green, **K**), where no difference was observed for NCSC clones (green, **G**).

Figure 3. Multipotency of NCSC and MSC from adult bone marrow

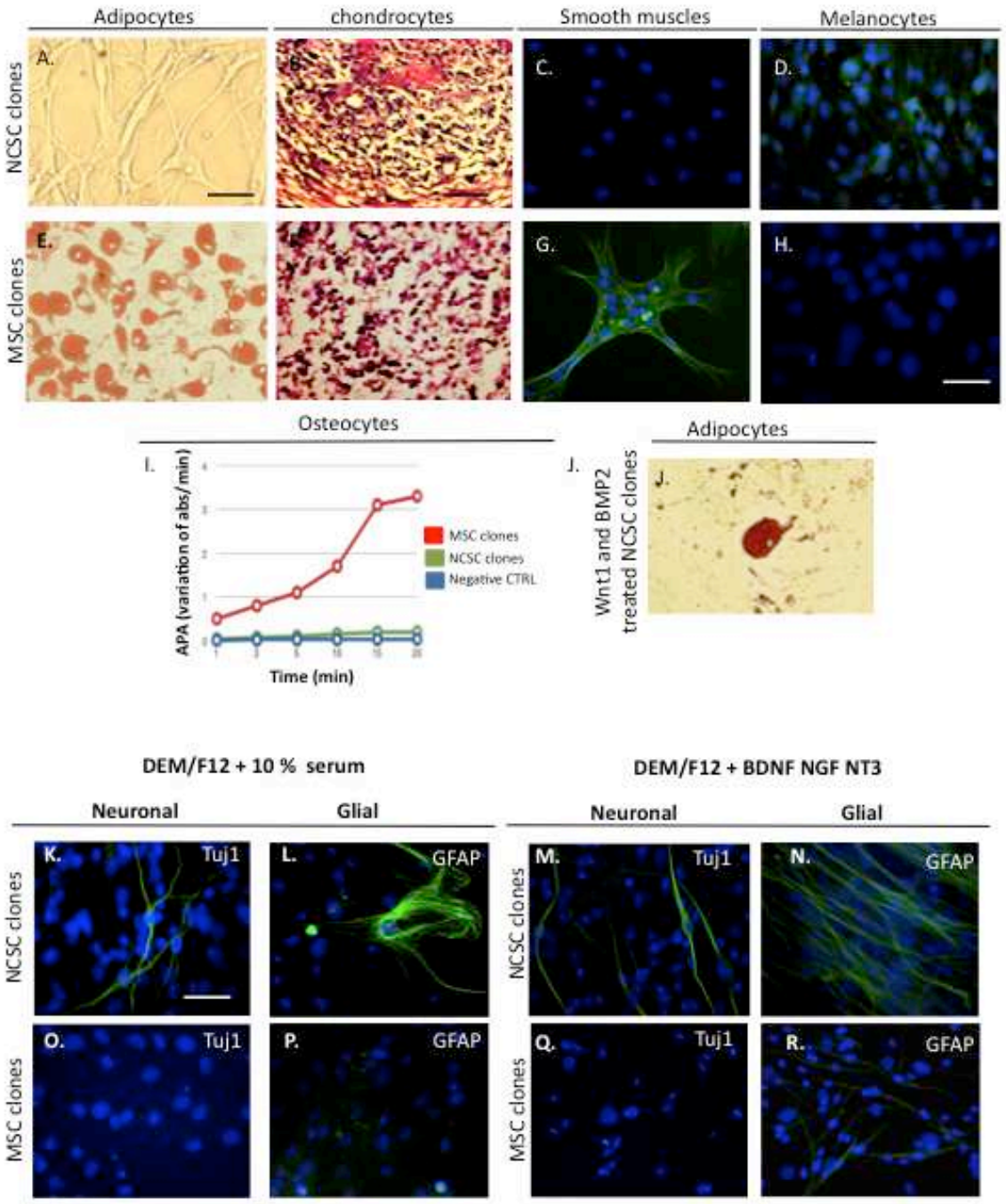

FIGURE 3. Multipotentcy of NCSC and MSC from adult bone marrow. NCSC clones were able to differentiate into chondrocytes (**B**) and melanocytes (**D**), but unable to differentiate into adipocytes (**A**) and Smooth muscle cells (**C**). Adipocytes are labeled with

Oil-Red O, chondrocytes with Blue toluidine, smooth muscle cells with anti-SMA and melanocytes with anti-Trp2 antibody. Likewise, only MSC clones were able to differentiate into osteocytes (**I**) quantified by the alkaline phosphatase activity measurement. Interestingly, when pre-treated with Wnt1 and BMP2, NCSC were able to differentiate into adipocytes (**J).** NCSC and MSC clones were cultivated for 10 days in serum-containing medium: DEM/F12 + 10 % FBS. In those conditions, NCSC clones were able to spontaneously differentiate into Tuj1- (green, **K**) and GFAP- (green, **L**) positive cells, where no differentiation was observed for MSC clones (**O,P**). We then placed NCSC and MSC clones in neurotrophin-containing medium (DEM/F12 + BDNF + NT3 + NGF). In those conditions, we obtained Tuj1- (green, **M**) and GFAP- (green, **N**) positive cells with NCSC clones, where only few GFAP-positive cells (green, **R**), but no Tuj1-positive cells (**Q**) were obtained with MSC clones. Nuclei were counterstained with Dapi (blue). Scale bars =30 μm. Scale bars B and F = 50 μm.

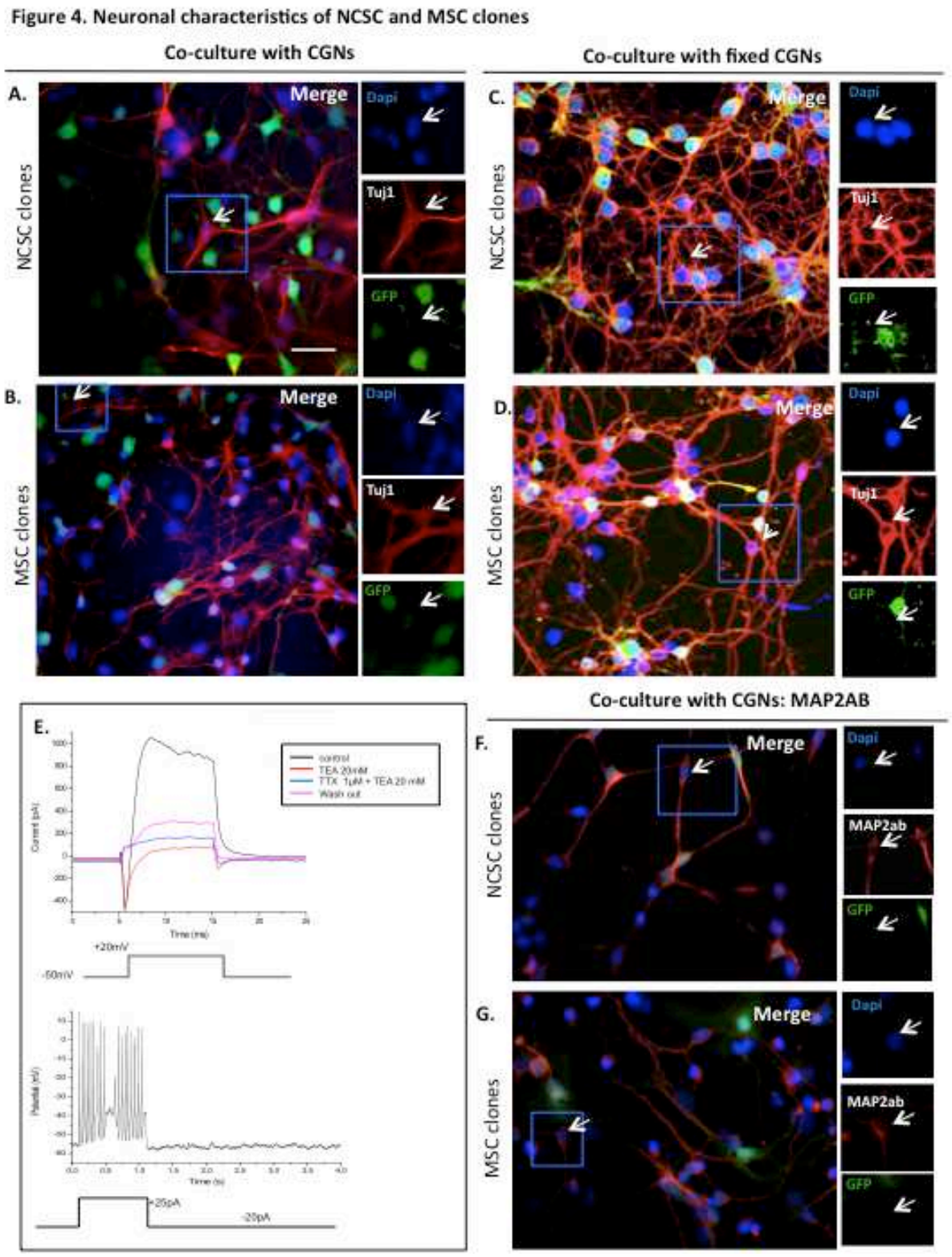

Figure 4. Neuronal characteristics of NCSC and MSC clones. NCSC and MSC clones were co-cultured for 5 days with green fluorescent protein (GFP)–positive

cerebellar granule neurons (CGNs, green). Interestingly, both sets of clones were able to differentiate into Tuj1-positive cells (red, **A** and **B**). Arrowheads show clonal cells that were Tuj1-psoitive (red), but GFP-negative (green) rejecting their CGNs origin. To determine if the presence of Tuj1-positive cells from MSC clones co-cultivated with CGNs, was due to cell fusion events or because of other requested factors expressed by CGNs, we co-cultivated NCSC clones and MSC clones with CGNs that have been cultivated for 5 days before being fixed with 4 % paraformaldehyde. Clones were cultivated on top of fixed CGNs in presence of CGNs conditioned medium for 7 days. Interestingly, we were still able to obtained Tuj1-positive cells with both NCSC and MSC, in those conditions (**C,D**). Whole-cell recordings were performed on co-cultivated NCSC or MSC, however, only 2% of MSC presented sodium voltage-gated channels and consequently action potentials. (**E**, upper part) Voltage-clamp recording in which the holding potential was transiently and repeatedly stepped from -50 mV to +20 mV under different conditions. Note the appearance of a fast inward tetrodotoxine (TTX)-sensitive current, followed by a slower outward current which was blocked by tetraethylammonium (TEA ; see colour-coding of the traces in the inset. (**E**, bottom part). Current-clamp experiment. A depolarizing current injection evoked a train of action potentiels in the same cell. Note that the cell was continuously hyperpolarized with a small amount of current (-20 pA). As action potentials were observed after 12 days, we performed a MAP2ab labelling on NCSC (**F**) and MSC (**G**) co-cultivated for 12 days with CGNs. Nuclei were counterstained with Dapi (blue). Scale bars =30 μm.

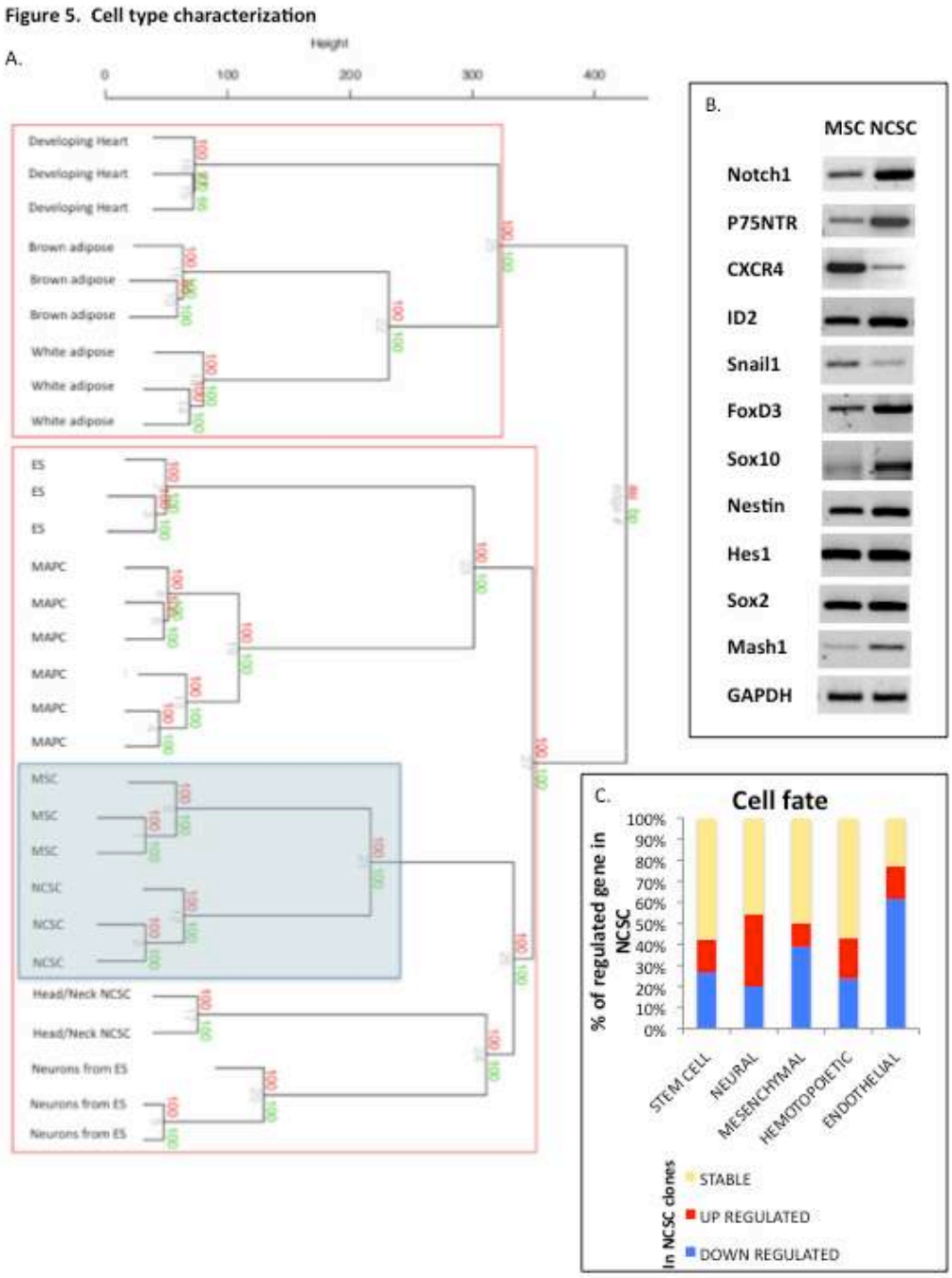

FIGURE 5. Microarray analyses of NCSC and MSC clones: Cell fate. **A.** Dendrogram generated after agglomerative hierarchical clustering using Euclidean distance, average linkage and multiscale bootstrap resampling. 29 expression array data sets were included in an unsupervised analysis with hierarchical clustering of samples. Adipocytes (brown and white adipose, GSE8044); cardiomyocytes (GSE7196); ES and neural precursors from ES (GSE8024); MAPC (GSE6291); head and neck neural crest stem cells (GSE11149) are accessible on GEO datasets / NCBI (http://www.ncbi.nlm.nih.gov/gds). All replicates were

merged under the same denomination when possible. The dendrogram was build with the Euclidean distance as dissimilarity metric and the average linkage method for definition of the structure. Values on the edges of the clustering are *p*-values (%). Red values are **AU** *p*-values, and green values are **BP** values. AU (Approximately Unbiased) *p*-values were computed by multiscale bootstrap resampling. BP (Bootstrap Probability) values were computed by normal bootstrap resampling. R-cran "pvclust" package was used for assessing the uncertainty of this hierarchical cluster analysis for 10000 permutations of genes. Those values indicated how strongly the cluster was supported by the data. **B.** Using semi-quantitative RT-PCR, we analyzed the expression of several genes known to be expressed in stem cells or neural crest cells (Primers and PCR characteristics can be found in Glejzer et al., [9]). **C.** In this figure, we reported all genes from microarray analyses that were expressed by NCSC or MSC clones, and involved in cell fate decision. We classified those genes in 5 families: stem cell, neural, hematopoietic, mesenchymal and endothelial fate. Those results suggested that NCSC clones mainly expressed neural genes while MSC clones mainly expressed mesenchymal and endothelial genes. Genes that were equally expressed by both cell types are in yellow, over-expressed genes in NCSC are in red and down-expressed genes in these cells are in blue.

Figure 6. Signaling pathways in NCSC and MSC clones

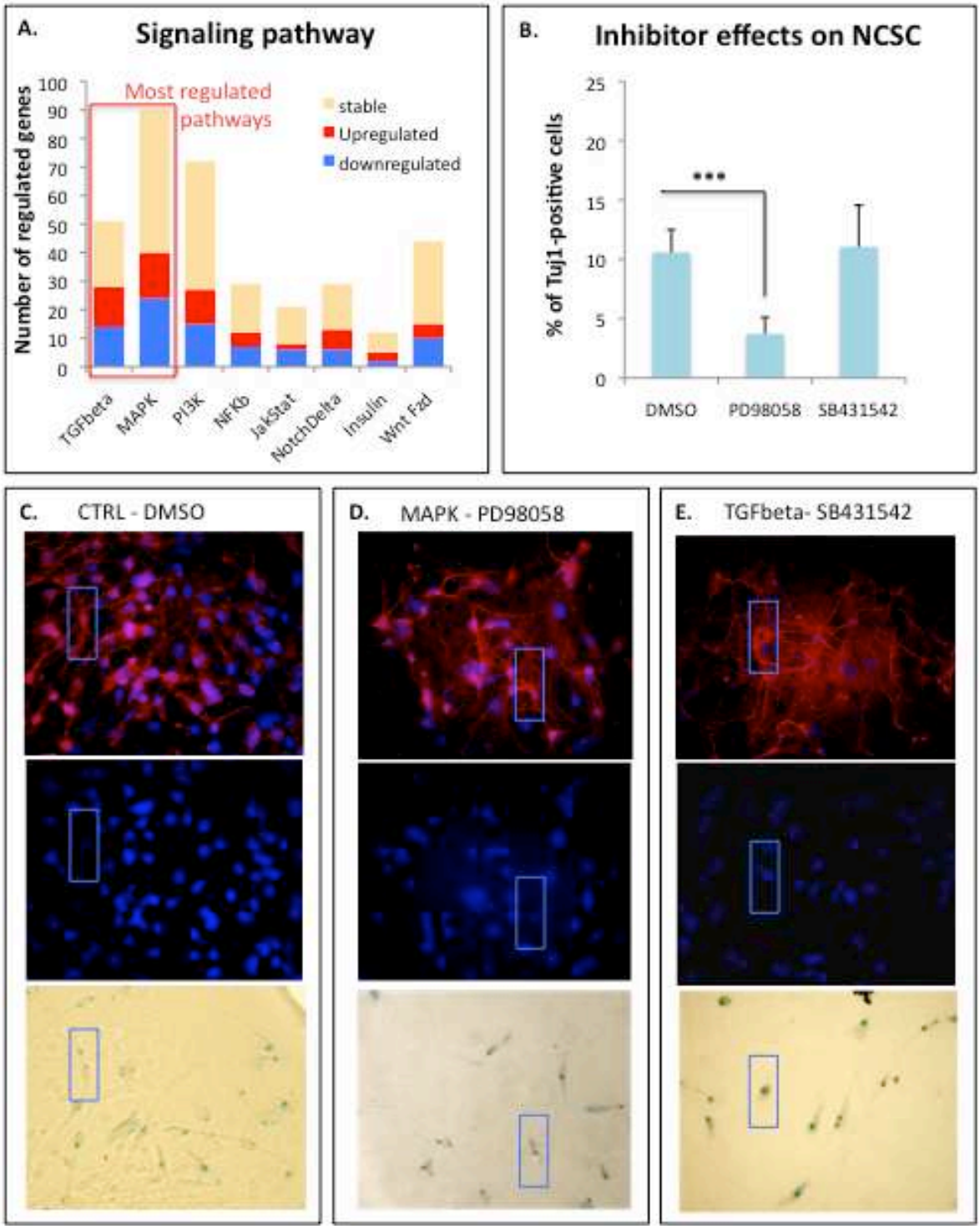

FIGURE 6. NCSC and MSC clones: Signaling Pathway. A. Starting from microarray results, we reported all genes that were expressed by NCSC clones or MSC clones, and involved in cell signaling. We classified those genes in 8 families: WNT/FZD,

NOTCH/DELTA, INSULIN, NFkB, MAPK, PI3K, JAK/STAT and TGFbeta. Looking at those results, it appeared that TGFbeta and MAPKinase were the two most regulated gene families in NCSC clones compared to MSC clones. **B.** We consequently analyzed their implication in neuronal differentiation of NCSC clones. We co-cultivated NCSC clones with cerebellar granule neurons in presence of PD98058 (MAPK inhibitor, 1 μM solubilised in DMSO) or SB431542 (TGFbeta inhibitor, 1 μM solubilised in DMSO) for 5 days. Inhibitor treatment started on day 0 and refreshed on day 3 of the co-culture. Compared to the control condition (DMSO), we observed a significant decrease of the number of Tuj1-postive cells in presence of PD98058, where no difference was observed in presence of SB431542 ($n = 2$, $p < 0.005$, one way ANOVA followed by Newman-Keuls post hoc test). **C-E.** NCSC clones were co-cultured for 5 days with cerebellar granule neurons (CGN), in presence of DMSO (C), PD98058 (D) or SB431542 (E). Numbers of beta-III tubulin- (Tuj1, red) and beta-galactosidase-positive cells were quantified attesting of the ability of NCSC clones to differentiate into neurons. Blue rectangle show an example of double positive cells for each population.

Table 1. 2D-DIGE: protein overexpresed in nestin (+) compare to nestin (-) BMSC

Symbol	Protein name	Location	Cell cycle influence
AHNAK	AHNAK nucleoprotein	Nucleus	-
ANXA5	annexin A5	Membrane	Proliferation
ANXA6	annexin A6	Membrane	-
ATIC	5-aminoimidazole-4-carboxamide ribonucl. formyltransferase	unknown	Proliferation
ATP5B	ATP synthase, H+ transporting 5B	Cytoplasm	-
ATP5H	ATP synthase, H+ transporting	Cytoplasm	-
C1QBP	complement component 1, q subcomponent binding protein	Cytoplasm	Proliferation
CALD1	caldesmon 1	Cytoplasm	Proliferation
CALR	calreticulin	Cytoplasm	Proliferation
CALU	calumenin	Cytoplasm	-
CAPNS1	calpain, small subunit 1	Cytoplasm	cell death
CCT4	chaperonin containing TCP1, subunit 4 (delta)	Cytoplasm	-
CKB	creatine kinase, brain	Cytoplasm	-
CNN3	calponin 3, acidic	Cytoplasm	-
CTSB	cathepsin B	Cytoplasm	-
CTSD	cathepsin D	Cytoplasm	-
DARS	aspartyl-tRNA synthetase	Cytoplasm	Proliferation
DLAT	dihydrolipoamide S-acetyltransferase	Cytoplasm	-
DPP7	dipeptidyl-peptidase 7	Cytoplasm	-
DPYSL2	dihydropyrimidinase-like 2	Cytoplasm	Proliferation
DPYSL3	dihydropyrimidinase-like 3	Cytoplasm	-
DYNC1LI1	dynein, cytoplasmic 1, light intermediate chain 1	Cytoplasm	-
EDF1	endothelial differentiation-related factor 1	Nucleus	-
EEF1A1	eukaryotic translation elongation factor 1 alpha 1	Cytoplasm	Proliferation
EEF2	eukaryotic translation elongation factor 2	Cytoplasm	Proliferation
EZR	ezrin	Membrane	-
FAM129A	family with sequence similarity 129, member A	unknown	-
FTH1	ferritin, heavy polypeptide 1	Cytoplasm	-
FTL	ferritin, light polypeptide	Cytoplasm	-
GFAP	glial fibrillary acidic protein	Cytoplasm	-
GNAQ	guanine nucleotide binding protein (G protein), q polypeptide	Membrane	cell death
HMOX1	heme oxygenase (decycling) 1	Cytoplasm	-
HNRNPK	heterogeneous nuclear ribonucleoprotein K	Nucleus	-
HSP90AB	heat shock protein 90kDa alpha (cytosolic), B 1	Cytoplasm	-
HSPA1B	heat shock 70kDa protein 1B	Cytoplasm	-
HSPB1	heat shock 27kDa protein 1	Cytoplasm	-
KLC1	kinesin light chain 1	Cytoplasm	-
MAP2	microtubule-associated protein 2	Cytoplasm	-
MSN	moesin	Membrane	cell death
NCOA2	nuclear receptor coactivator 2	Nucleus	-
NEDD4	neural precursor cell expressed, development. down-regul. 4	Cytoplasm	-
NUCB2	nucleobindin 2	Nucleus	-
P4HA1	prolyl 4-hydroxylase, alpha polypeptide I	Cytoplasm	cell death
PAK2	p21 protein (Cdc42/Rac)-activated kinase 2	Cytoplasm	cell death
PCNA	proliferating cell nuclear antigen	Nucleus	Proliferation
PDCD6IP	programmed cell death 6 interacting protein	Cytoplasm	cell death
PDIA2	protein disulfide isomerase family A, member 2	Cytoplasm	-
PDIA3	protein disulfide isomerase family A, member 3	Cytoplasm	cell death
PDIA6	protein disulfide isomerase family A, member 6	Cytoplasm	-
PDK2	pyruvate dehydrogenase kinase, isozyme 2	Cytoplasm	-
POLA1	polymerase (DNA directed), alpha 1, catalytic subunit	Nucleus	Proliferation
PRDX3	peroxiredoxin 3	Cytoplasm	cell death
RAB1A	RAB1A, member RAS oncogene family	Cytoplasm	-
RAB2A	RAB2A, member RAS oncogene family	Cytoplasm	-
RAB6A	RAB6A, member RAS oncogene family	Cytoplasm	-
RENBP	renin binding protein	unknown	
RNPEP	arginyl aminopeptidase (aminopeptidase B)	Cytoplasm	
ROCK2	Rho-associated, coiled-coil containing protein kinase 2	Cytoplasm	Proliferation
RPS6KA1	ribosomal protein S6 kinase, 90kDa, polypeptide 1	Cytoplasm	-
SARDH	sarcosine dehydrogenase	Cytoplasm	-
SH3GL1	SH3-domain GRB2-like 1	Cytoplasm	-
SOD1	superoxide dismutase 1, soluble	Cytoplasm	Proliferation
SPARC	secreted protein, acidic, cysteine-rich (osteonectin)	Extracellular	Proliferation
STK3	serine/threonine kinase 3 (STE20 homolog, yeast)	Cytoplasm	-
TPM3	tropomyosin 3	Cytoplasm	Proliferation
TPM4	tropomyosin 4	Cytoplasm	Proliferation
TXNL1	thioredoxin-like 1	Cytoplasm	cell death
VAMP1	vesicle-associated membrane protein 1 (synaptobrevin 1)	Membrane	-
VCP	valosin-containing protein	Cytoplasm	Proliferation
YWHAE	tryptophan 5-monooxygenase activation protein, epsilon	Cytoplasm	Proliferation
YWHAG	tryptophan 5-monooxygenase activation protein, gamma	Cytoplasm	Proliferation
YWHAZ	tryptophan 5-monooxygenase activation protein, zeta	Cytoplasm	-